

# BEAM OPTICS STUDY FOR A POTENTIAL VHEE BEAM DELIVERY SYSTEM

C. S. Robertson\*, P. N. Burrows, M. Dosanjh<sup>1</sup>, University of Oxford, Oxford, UK  
 A. Latina, CERN, Geneva, Switzerland  
 A. Gerbershagen<sup>1</sup>, PARTREC, UMCG, University of Groningen, Netherlands  
<sup>1</sup>also at CERN, Geneva, Switzerland

## Abstract

VHEE (Very High Energy Electron) therapy can be superior to conventional radiotherapy for the treatment of deep seated tumours, whilst not necessarily requiring the space and cost of proton or heavy ion facilities. Developments in high gradient RF technology have allowed electrons to be accelerated to VHEE energies in a compact space, meaning that treatment could be possible with a shorter linac. A crucial component of VHEE treatment is the transfer of the beam from accelerator to patient. This is required to magnify the beam to cover the transverse extent of the tumour, whilst ensuring a uniform beam distribution. Two principle methodologies for the design of a compact transfer line are presented. The first of these is based upon a quadrupole lattice and optical magnification of beam size. A minimisation algorithm is used to enforce certain criteria on the beam distribution at the patient, defining the lattice through an automated routine. Separately, a dual scattering-foil based system is also presented, which uses similar algorithms for the optimisation of the foil geometry in order to achieve the desired beam shape at the patient location.

## INTRODUCTION AND BACKGROUND

### *Current Modalities of Radiotherapy*

Radiotherapy (RT) is an essential component of cancer treatment, required by 50% of patients [1]. In RT, a treatment beam is used to damage the DNA of the tumour cells and cause cell death. The main goal of RT is to cause as much damage to the tumour as possible, whilst reducing dose to any surrounding healthy tissue. This is known as increasing the “Therapeutic Window”. This is most critical when the tumour is seated deep within a patient, as organs particularly susceptible to radiation may be traversed. The dose deposition profile from an RT beam is dependent on the particle used for treatment [2]. Modern techniques in conventional (X-ray) RT have been developed to reduce dose to healthy tissues longitudinally and laterally [3]. Hadron beams can provide more precise treatments with less dose to healthy tissues than conventional RT due to the Bragg peak [2]. They can also be manipulated directly with magnets to allow scanning of the beam across the tumour. As such, they are very well suited for the treatment of deep-seated tumours. Hadron treatment facilities are however much larger and more expensive than conventional RT facilities [4]. This is due to the requirement for cyclotrons or

synchrotrons for acceleration rather than the small LINACs used for conventional RT, extended shielding requirements as well as the much larger gantries for bending the higher rigidity hadron beams.

### *VHEE*

A promising modality for RT is VHEE (Very High Energy Electron) therapy. These are defined as electron beams with energies above 50 MeV, and would be capable of reaching deep-seated tumours [5]. There is evidence that VHEE beams would be less sensitive to inhomogeneities in the patient tissues than hadron beams. With the implementation of scanning and/or focusing, VHEE beams could also provide superior tumour conformity and avoidance of healthy tissues compared to conventional RT [6, 7]. Two crucial advantages that VHEE would have over hadron therapy are the required cost and space. A 200 MeV electron beam would require weaker magnets and/or a more compact gantry for delivering treatment. Developments in high gradient X-band RF-technology have also allowed the possibility of electrons being accelerated to VHEE energies in a very compact LINAC [8]. This would require less space than the circular accelerators used for hadron therapy.

### *Aim*

The aim of this work is to design a transfer line for a 100 MeV VHEE beam from acceleration to the patient, using a simple model. This is an exploration and verification of the methodology for this design process, rather than a fully practical implementation. The beam should meet certain requirements for treatment whilst also being compact and efficiently designed to minimise associated costs.

### *Initial Conditions and Beamline Geometry*

The gantry was based upon a “Riesenrad” style gantry, consisting of a beamline with a single dipole [9]. This gantry would be rotated along with the patient couch to allow irradiation from multiple angles, shown in Fig. 1. The initial beam was assumed to have a uniform transverse distribution with a radius of 1 mm, an angular divergence of 1 mrad, and a momentum spread of 0.25%. It was required to be magnified to the radius of a large tumour - here taken to be between 50 mm and 100 mm. Furthermore, the beam was required have a uniform transverse distribution to ensure an even dose across the tumour. The study of scanned and focused beam delivery was left for future work. Achromaticity of the beamline whilst desirable for symmetry in both

\* cameron.robertson@physics.ox.ac.uk

transverse axes was not a key aim of the design processes at this stage, but instead the physical beam profile was the most fundamental consideration.

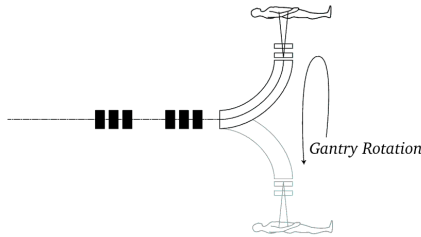


Figure 1: Riesenrad Gantry concept [9]

## METHOD AND RESULTS

### Magnification Optics

The first method for developing the gantry was based around a lattice of quadrupoles. This was carried out using Nelder-Mead [10] (simplex) minimisation with RF-Track, a code developed at CERN [11]. The optimisation process was carried out using a merit function to characterise the transverse beam distribution at the patient. The merit function is composed of a sum of weighted terms, summarised by

$$M = \omega_1 M_{\text{mean}} + \omega_2 M_{\text{mag}} + \omega_3 M_{\text{kurtosis}} \quad (1)$$

for each transverse dimension.  $M_{\text{mean}}$  and  $M_{\text{mag}}$  are terms which are minimal when the distribution at the patient is centred and magnified to a defined radius, respectively.  $M_{\text{kurtosis}}$  is minimised when the beam has a constant transverse distribution across this radius, and is found using the kurtosis (tailedness) of the beam [12]. The weights in the merit function were determined through iterative investigation of optimisation results, attempting to balance these values for the desired final distribution.

The minimisation for this function was carried out using the gradients and positions of a number of quadrupole magnets as variables, along with the pole tip face angles of the single dipole. Limits were enforced on the strengths of the quadrupole magnets with respect to the required beam apertures to ensure magnetic fields below saturation for resistive magnets. At the end of the gantry, a 2 m long space was assumed to leave room for beam diagnostics and additional optics. The number of quadrupole magnets was to be kept to a minimum – particularly those downstream of the dipole as these would significantly add to the total cost of the gantry due to their required rotation. The optimisation was run a significant number of times with random seeds being used for input variables within the described bounds. This was necessary since the Nelder-Mead method is susceptible to returning local minima. The solution deemed most successful is presented here, with the gantry layout and quadrupole strengths as well as the resultant transverse distribution in the patient displayed in Fig. 2. Excellent consistency across the final beam out to 75 mm was achieved, with negligible

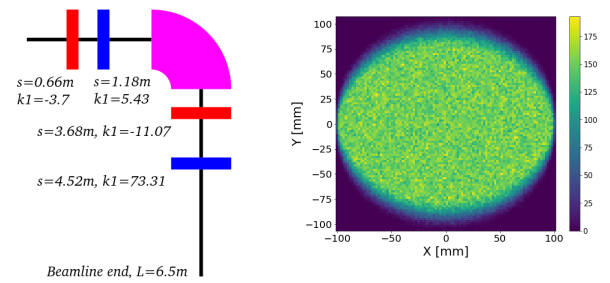


Figure 2: Magnification optics layout (left) and transverse beam distribution at patient location without collimation (right), colour represents density in arbitrary units

large scale variation, corresponding to a kurtosis value of 2.000 in X and 2.004 in Y (the bending axis). After collimation out to 75 mm to retain only the flat region, 61% of the initial beam was retained. The rather large losses from collimation are due to the asymmetry between the transverse axes caused by dispersion.

### Dual Scattering Foil

The second method of beam magnification proposed was the use of a dual scattering foil. The general principle of this is to firstly magnify a pencil beam by sending it through a flat scattering foil. The scattering process is random and

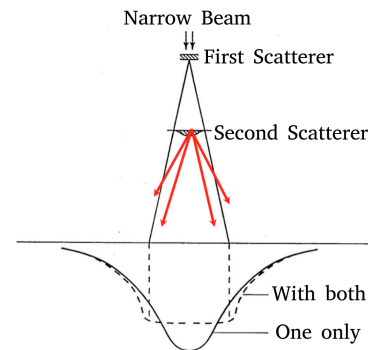


Figure 3: Dual Scattering Foil Concept [13]

thus the magnified beam will have an approximately Gaussian transverse distribution. A 2nd scatterer with a more complex shape is then used to correct the Gaussian beam into a flat beam for treatment. This shape would be Gaussian to complement the beam, preferentially scattering the denser centre of the beam over the total beam radius. This concept is shown in Fig. 3.

To reduce particle production and associated energy losses as well as limiting divergence, a distance of 2.5 m between the 1st scatterer and the patient was enforced for this gantry. The two quadrupoles upstream of the dipole in the magnification optics design were retained for this setup in order to constrain the beam travelling through the dipole. The 1st scatterer was chosen to be composed of tantalum, as TOPAS [14, 15] simulations demonstrated a higher efficiency of scattering angle increase against photon production for high Z

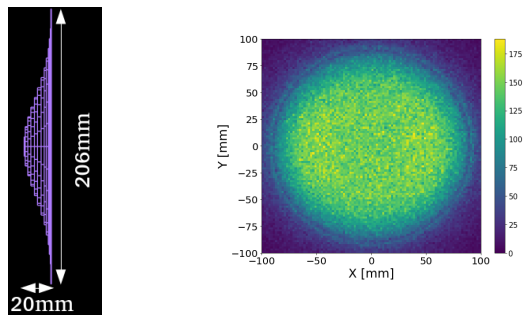


Figure 4: 2nd scatterer visualisation (left) and transverse beam density distribution at patient without collimation (right), colour represents density in arbitrary units

materials. Very high precision machining would be required for manufacturing a tantalum 2nd scatterer as it would be very thin. A much thicker, low Z material such as plastic would have more photon production however. Aluminium was chosen as a compromise between these two extremes.

The same minimisation principle was utilised for optimisation of the foils. The geometry of the system was used as the variable in the optimisation. More precisely, the longitudinal thickness of the first scatterer, and the amplitude and standard deviation determining the shape of the 2nd, Gaussian scatterer were used as the input parameters along with the longitudinal position of the 2nd scatterer relative to the 1st. RF-Track and TOPAS were used in conjunction to carry out the simulations for this process. The same merit function as shown in Eq. 1 was again minimised from many random distributions of these variables. The optimum 2nd scatterer geometry is shown in Fig. 4, along with the resultant transverse beam distribution in the patient. A constant transverse beam distribution with a radius of 60 mm was achieved, with consistency of 94% in the transverse distribution density in this range. The corresponded to a kurtosis value of 2.021 in X and 1.985 in Y. This collimation to remove the more widely scattered particles was rather significant, and thus transmission through the dual scattering system with collimation was 55%.

## DISCUSSION

### Comparison

Particularly in the case of the magnification optics method, the arrangement and strengths of the magnets would be crucial. Small alignment errors and beam jitter could have detrimental effects to the final beam. This method is also heavily dependent on the initial beam distribution, and one cannot assume that the same optics setup with a more realistic beam would provide a similar result. Even when minimised as far as possible as in this work, the beam at the patient still had a dose of X-rays that was comparable to that of the electrons for the dual scattering method. Enforcing the 2.5 m length between the 1st scatterer and the patient resulted in a large minimum gantry size. A solution to the above issues could involve making the first foil thicker and

reducing the distance between it and the second foils, or moving the foils upstream of the single dipole; the concern for the latter would be that the scattering system increases the energy spread of the beam, and thus increases the effects of dispersion. This would also require a dipole magnet with a large aperture.

The dual scattering foil system while likely cheaper and easier to implement would always have the unavoidable issues of particle production compared to the pure VHEE beam from the magnification optics. However, the problems caused by misalignment and gantry rotation would likely be more severe for the magnification optics solution due to the increased weight and number of required beamline elements.

### Future Work

An valuable extension to this study would be a quantitative study of the effects of misalignment on the final distribution, for both methods. This could involve additional optimisations of a static setup to account for variations in the initial beam. The above magnification optics setup shown in Fig. 2 could be kept static and only the strengths of the magnets varied to be used as a transfer line for different distributions. One would expect that the foil system would be less dependent on the initial beam than the optics method, but this would also need to be quantified explicitly.

The impact of the X-ray production from the dual scattering foil on the patient dose distribution will require further study and comparison to the “pure” VHEE beam from the magnification optics. Due to the (relatively) high energy of the electrons, the details and method of collimation should also simulated for this study of dose in the patient. Monte-Carlo codes such as TOPAS and FLUKA [16, 17] could be used for this. Furthermore, the maximum achievable radius of the constant beam at the patient appeared to be somewhat limited by enforcing the strictly Gaussian shape of the 2nd scatterer. A more flexible approach allowing for non-Gaussian aberrations in the shape design could allow this to be solved.

## CONCLUSION

Two general concepts were shown to explore methodologies for design of a VHEE treatment line, using an idealised initial beam distribution and Riesenrad treatment gantry. The first, using a lattice of quadrupoles, allowed a pure VHEE beam to be magnified and flattened with a relatively small gantry radius. The second, using a dual scattering foil system, also achieved this magnification and flattening, although this also resulted in unavoidable extra particle production from the beam-matter introduction. This was minimised by situating the system significantly upstream of the patient, although this led to a larger gantry radius. Both beamline designs were carried out using multiple simplex minimisation routines with random seeding. Future work will involve carrying out design studies with different initial beam distributions and studies of lattice imperfections.

## REFERENCES

- [1] J. M. Borrás *et al.*, “How many new cancer patients in Europe will require radiotherapy by 2025? An ESTRO-HERO analysis,” *Radiotherapy and Oncology*, vol. 119, no. 1, pp. 5–11, 2016, doi:10.1016/j.radonc.2016.02.016
- [2] T.-Z. Yuan, Z.-J. Zhan, and C.-N. Qian, “New frontiers in proton therapy: applications in cancers,” *Cancer Communications*, vol. 39, no. 1, pp. 1–7, 2019, doi:10.1186/s40880-019-0407-3
- [3] P. P. Connell and S. Hellman, “Advances in Radiotherapy and Implications for the Next Century: A Historical Perspective,” *Cancer Research*, vol. 69, no. 2, pp. 383–392, 2009, doi:10.1158/0008-5472.can-07-6871
- [4] R. Amos *et al.*, “Proton Beam Therapy – the Challenges of Delivering High-quality Evidence of Clinical Benefit,” *Clinical Oncology*, vol. 30, no. 5, pp. 280–284, 2018, Proton Beam and Particle Therapy, doi:10.1016/j.clon.2018.02.031
- [5] C. DesRosiers, V. Moskvina, A. F. Bielajew, and L. Papiez, “150-250 MeV electron beams in radiation therapy,” *Physics in Medicine & Biology*, vol. 45, no. 7, pp. 1781–1805, 2000, doi:10.1088/0031-9155/45/7/306
- [6] E. Schüler *et al.*, “Very high-energy electron (VHEE) beams in radiation therapy; Treatment plan comparison between VHEE, VMAT, and PPBS,” *Medical physics*, vol. 44, no. 6, pp. 2544–2555, 2017, doi:10.1002/mp.12233
- [7] B. Palma *et al.*, “Assessment of the quality of very high-energy electron radiotherapy planning,” *Radiotherapy and Oncology*, vol. 119, no. 1, pp. 154–158, 2016, doi:10.1016/j.radonc.2016.01.017
- [8] M. G. Ronga *et al.*, “Back to the Future: Very High-Energy Electrons (VHEEs) and Their Potential Application in Radiation Therapy,” *Cancers*, vol. 13, no. 19, 2021, doi:10.1016/j.radonc.2016.01.017
- [9] H. Owen, D. Holder, J. Alonso, and R. Mackay, “Technologies for Delivery of Proton and Ion Beams for Radiotherapy,” *International Journal of Modern Physics A*, vol. 29, no. 14, 2013, doi:10.1142/S0217751X14410024
- [10] D. M. Olsson and L. S. Nelson, “The Nelder-Mead simplex procedure for function minimization,” *Technometrics*, vol. 17, no. 1, pp. 45–51, 1975, doi:10.1080/00401706.1975.10489269
- [11] A. Latina, *RF-Track Reference Manual*, version 2.0.4, 2020, doi:10.5281/zenodo.3887085
- [12] K. P. Balanda and H. L. MacGillivray, “Kurtosis: A Critical Review,” *The American Statistician*, vol. 42, no. 2, pp. 111–119, 1988, doi:10.2307/2684482
- [13] J. D. LeBlanc, “Design of electron dual foil scattering systems for Elekta Infinity radiotherapy accelerators,” 2012, doi:10.31390/gradschool\_theses.2440
- [14] J. Perl, J. Shin, J. Schumann, B. Faddegon, and H. Paganetti, “TOPAS: an innovative proton Monte Carlo platform for research and clinical applications,” *Medical physics*, vol. 39, no. 11, pp. 6818–6837, 2012, doi:10.1118/1.4758060
- [15] B. Faddegon *et al.*, “The TOPAS tool for particle simulation, a Monte Carlo simulation tool for physics, biology and clinical research,” *Physica Medica*, vol. 72, pp. 114–121, 2020, doi:10.1016/j.ejmp.2020.03.019
- [16] C. Ahdida *et al.*, “New Capabilities of the FLUKA Multi-Purpose Code,” *Front. Phys.*, vol. 9, 2022, doi:10.3389/fphy.2021.788253
- [17] G. Battistoni *et al.*, “Overview of the FLUKA code,” *Annals of Nuclear Energy*, vol. 82, pp. 10–18, 2015, Joint International Conference on Supercomputing in Nuclear Applications and Monte Carlo 2013, SNA + MC 2013. Pluri- and Trans-disciplinarity, Towards New Modeling and Numerical Simulation Paradigms, doi:10.1016/j.anucene.2014.11.007